

## Electric Fields that “Arrive” before the Time Derivative of the Magnetic Field prior to Major Earthquakes

P. A. Varotsos,<sup>1,2,\*</sup> N. V. Sarlis,<sup>1</sup> and E. S. Skordas<sup>1,2</sup>

<sup>1</sup>*Solid State Section, Physics Department, University of Athens, Panepistimiopolis, Zografos 157 84, Athens, Greece*

<sup>2</sup>*Solid Earth Physics Institute, Physics Department, University of Athens, Panepistimiopolis, Zografos 157 84, Athens, Greece*

(Received 12 February 2003; published 3 October 2003)

The low frequency electric signals (emitted from the focal area when the stress reaches a *critical* value) that precede major earthquakes, are recorded at distances  $\approx 100$  km being accompanied by magnetic field variations. The electric field “arrives” 1 to 2 *s* before the time derivative of the horizontal magnetic field. An explanation, which is still awaiting, should consider, beyond *criticality*, the large spatial scale as well as that the transmission of the electromagnetic fields (through an inhomogeneous weakly conductive medium like the Earth) obeys diffusion type equations.

DOI: 10.1103/PhysRevLett.91.148501

PACS numbers: 91.30.-f, 03.50.De, 05.40.-a, 41.20.-q

This Letter presents experimental results, which show that low frequency ( $\leq 1$  Hz) electric signals, when transmitted in an inhomogeneous weakly conductive dielectric medium like the Earth, are recorded at distances of the order of 100 km 1 to 2 sec *before* the associated magnetic field variations (concerning the latter, what was directly measured was the time derivative  $d\mathbf{B}/dt$  and not the magnetic field  $\mathbf{B}$ ). Such a time difference has never been reported before, probably due to the large (spatial) scale of the experiment under consideration (i.e., the distance between the emitting source and the measuring site). The signals analyzed are the so-called seismic electric signals (SES) activities (consisting of hundreds of pulses), which have been found in Greece [1,2] and Japan [3] to precede earthquakes (EQs) from several hours to a few months [2,4]. Several physical mechanisms for the SES’s generation have been proposed [4,5], e.g., it has been suggested [4] that these signals are emitted when the stress reaches a *critical* value in the focal area. Actually, it was recently shown [6] that these signals exhibit long-range correlations consistent with critical behavior.

We first summarize the instrumentation. The magnetic field variations are measured by three DANSK coil magnetometers (DMM), oriented along the three axes: EW, NS, and vertical. Their calibration, described in detail elsewhere [7,8], shows that they act as  $d\mathbf{B}/dt$  detectors for periods larger than around half a second. Furthermore, their output is “neutralized” approximately 200 ms after the “arrival” of a Heaviside unit step magnetic variation. In other words, a signal recorded by these magnetometers should correspond to a magnetic variation that has “arrived” at the sensor less than 200 ms before the recording [7]. Concerning the (horizontal) electric field  $\mathbf{E}$  variations, they are monitored by measuring the variation  $\Delta V$  of the potential difference between (pairs of) electrodes—measuring dipoles—grounded at depths of  $\approx 2$  m. Several such dipoles [8] are deployed usually along two directions (e.g., EW and NS) with lengths a

few to several tens of meters (short-dipoles) or a couple of kilometers (long dipoles). The data of both fields  $\mathbf{E}$ ,  $\mathbf{B}$  were simultaneously collected (1 sample/sec) by the *same* acquisition system (Campbell 21X Datalogger). Low pass 10 Hz (1 Hz) filters were only used in the electric field measurements for the short (long) dipoles.

The following two points have been assured [7]: First, for the usual artificial noises (i.e., electrical disturbances due to nearby operating man-made sources, e.g., [6]), the measured electric variations “arrive simultaneously” (i.e., with a time difference appreciably smaller than 1 sec) with the magnetic ones detected by DMM. Second, for the so-called magnetotelluric (MT) disturbances, which are induced by small changes of the Earth’s magnetic field, for periods  $T$  larger than 1 sec, the DMM recordings markedly precede the electric ones [8]. This is expected for changes of inductive nature, if we recall that, for  $T \geq 0.5$  sec, the DMM act as  $d\mathbf{B}/dt$  detectors (cf. assuming plane waves arriving at the Earth’s surface, for a uniform conductive half-space,  $E_x$  for example leads  $B_y$  in phase by  $45^\circ$ , e.g., [9]).

In what follows, we deal with the variations of the electric and magnetic field associated with SES activities. As an example, we consider the case of the 6.6 EQ that occurred in Greece at  $40.2^\circ$  N  $21.7^\circ$  E, on May 13, 1995. This was preceded [2] by two strong SES activities recorded at Ioannina station (IOA) (i.e., at a distance of around 80 km from the epicenter) on April 18 and 19, 1995. The former is shown in [8], while the latter is depicted in Fig. 1. The following five electric channels are shown in Fig. 1(a): two short electric dipoles at site “c” of length 50 m (labeled  $N_c-S_c$  and  $E_c-W_c$ ), while the upper three channels correspond to three long dipoles ( $L$ ,  $L'$ , and  $L'_s - I$ ) with lengths  $\approx 2, 2$  and 5 km, respectively (for the exact sites of the electrodes see [8]). The recordings  $V_m$  of the two horizontal DMM, labeled  $B_{NS}$  and  $B_{EW}$ , are shown in Fig. 1(b). This figure reveals that there are obvious magnetic disturbances at DMM, which accompanied the SES activities.

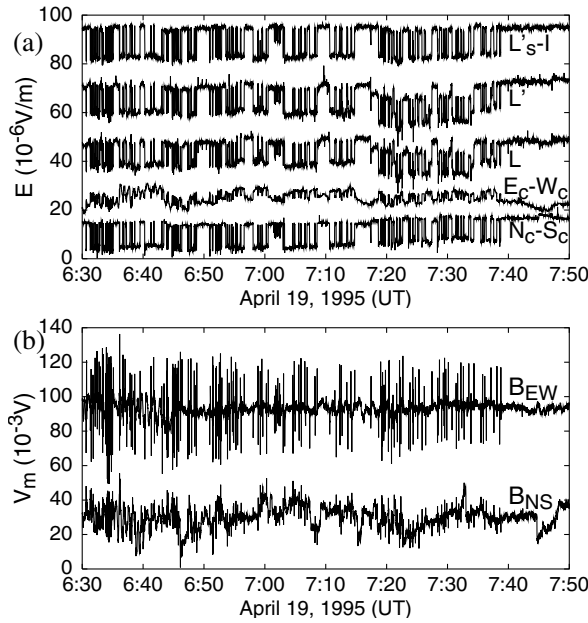


FIG. 1. The SES activity recorded at the station IOA on April 19, 1995 (a): Electric field, (b): Magnetic field variations; for the scale of  $V_m$ , 20 mV correspond [7] to a constantly increasing magnetic variation with  $dB/dt = 0.1$  nT/sec.

We now focus on the time difference  $\Delta t$  between the (arrival times of the) electric field variations and the associated magnetic ones. Figure 2(a) depicts the cross-correlation coefficient (“cr” values [8]), calculated between the time series of the electromagnetic fields versus  $\Delta t$ . In each case, one component of the electric field and one component of the horizontal DMM was used. An inspection of these results for the SES activity on April 19, 1995, reveals that the electric field variations precede the magnetic ones by  $\Delta t$  around 1–2 sec, which is appreciably larger than the time ( $\approx 0.2$  sec) determined in the calibration [7,8] of DMM to neutralize its output. The same  $\Delta t$  values are obtained [8] from the data analysis of the SES activity on April 18, 1995, or when studying the cr values of portions of the SES activities on April 18 or April 19. This fact, along with the large number (several hundreds) of pulses recorded, provides convincing evidence that the value  $\Delta t = 1 \sim 2$  sec is actually observed, despite the small sampling rate (1 Hz).

A question arises whether  $\Delta t$  is solely due to either the initiation or the decay of the aforementioned pulses. In order to discriminate this point, we first notice that — in view of their polarity [see Fig. 1(a)] — a negative derivative (Dt) of the  $E$ -field variation marks an initiation of a pulse, while a positive Dt a cessation. Thus, the cr values have been calculated [8] between the time-series of: (i) Dt of each one of the components of the  $E$  field and (ii) each one of the recordings of the two horizontal DMM. The same  $\Delta t$  values are obtained considering the time series of either positive or negative Dt values, Fig. 2(b).

In order to exclude the possibility that the above  $\Delta t$  values could have arisen from the measuring system, we

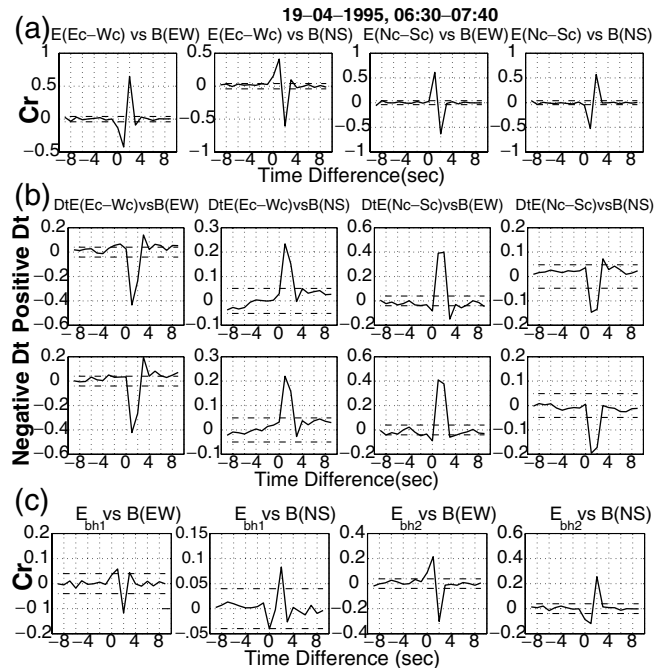


FIG. 2. (a) The cr values between one  $E$  component and one  $B$  component versus  $\Delta t$ , for the SES activity on April 19, 1995, after prewhitening [8]. The broken horizontal lines correspond to the 99% confidence level, indicating that the correlations at  $\Delta t = 1 \sim 2$  sec are statistically significant. (b) The cr values between the time series of either the positive Dt (first row) or the negative Dt (second row) of one  $E$ -field component and one  $B$ -field component. (c) the cr values after prewhitening, using the measurements in boreholes.

investigated the response of the latter to several MT variations recorded just before and after the SES activities. The corresponding cr values [8,10] show that the DMM recordings precede the electric ones, i.e., the *opposite* behavior than that in the case of the SES activities.

The  $\Delta t$  value is not significantly affected by the orientation (as well as the length) of the measuring electric dipoles. This becomes clear from a study of Fig. 3, which shows a 50 s excerpt from the records. In addition to the five electric dipoles mentioned in Fig. 1(a), recordings of the following five are shown: (i) Two short-dipoles  $E_b-W_b$ ,  $N_b-S_b$  installed at site “b” (which lies [8] 300 m far from the site c). (ii) Two dipoles  $E_b-W_b(-22^\circ)$ ,  $N_b-S_b(-22^\circ)$  installed at the same site b, but oriented along directions resulting from a rotation of the EW and NS by  $22^\circ$  anticlockwise, and (iii) an electric dipole, labeled  $E_{bh2}$ , of length  $L = 50$  m installed in a borehole [8] bh2 lying  $\approx 100$  m SE of site c (cf. similar values were measured in an independent [8] borehole bh1 lying  $\approx 100$  m NE of site c). Figure 2(c) shows that the  $E$ -fields measured in the boreholes also precede by  $\Delta t = 1 \sim 2$  sec the  $B$ -field components. The same  $\Delta t$  value is obtained [8] for all the other electric dipoles depicted in Fig. 3.

Finally, we emphasize that the  $\Delta t$  values reported in this Letter do not concern the electric and magnetic field disturbances that are associated with the arrival of

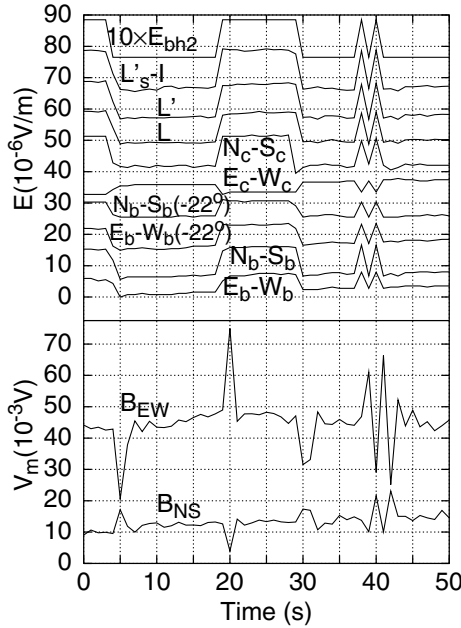


FIG. 3. A 50 s excerpt of the SES activity recorded at the station IOA on April 19, 1995. Measurements in horizontal and in borehole electric dipoles (cf. the latter is multiplied by 10) depicted along with those of the magnetic field.

seismic waves at the measuring site. The study of such disturbances, a preliminary version of which was reported in [11], will be presented in detail elsewhere.

The main result of the present Letter is that, at epicentral distances of the order of 100 km, the SES electric field precedes the time derivative of the magnetic field by  $\Delta t$  of the order of 1 sec. The explanation of such a difference should consider, in principle, that: (a) the fields follow diffusion type equations [12] (according to which the maximum of an electric impulse “needs” a time  $t \approx 1$  sec to “travel” a distance  $d$  of the order of 100 km in a conductive homogeneous medium having conductivity  $\sigma$  comparable to that of the Earth’s crust; in general,  $t$  scales with  $\sigma d^2$  [12]) and (b) the SES transmission model [4]; this suggests that the SES emitting electric dipole source lies in the vicinity of (and is oriented almost perpendicular [13] to) a conductive path of conductivity  $\sigma_p$ , which terminates below the Earth’s surface close to the measuring station (the existence of such a path is supported by recent detailed MT measurements at IOA [8,9]). The electric field values are then enhanced [14] near the termination of the path (*edge effects*). Numerical solutions of this model have been already published in the frequency domain [15]. Analytical solutions can be also achieved, but for the simple case of a conductive cylindrical path of infinite extent embedded in a less conductive medium when the electric dipole source coincides with the cylinder axis. We now turn to the discussion of this case.

In linear passive media, the electromagnetic fields can be expressed in terms of the source current density  $\mathbf{j}(\mathbf{r}, t)$

by using the tensor Green’s functions  $\vec{g}_E(\mathbf{r}, \mathbf{r}'; t - t')$ ,  $\vec{g}_B(\mathbf{r}, \mathbf{r}'; t - t')$  for the electric and magnetic field, respectively. Applying the convolution theorem we find

$$\mathbf{E}(\mathbf{r}, \omega) = \int_{V'} \vec{G}_E(\mathbf{r}, \mathbf{r}'; \omega) \cdot \mathbf{J}(\mathbf{r}', \omega) d^3 \mathbf{r}', \quad (1)$$

$$\mathbf{B}(\mathbf{r}, \omega) = \int_{V'} \vec{G}_B(\mathbf{r}, \mathbf{r}'; \omega) \cdot \mathbf{J}(\mathbf{r}', \omega) d^3 \mathbf{r}', \quad (2)$$

for the Fourier transforms  $\mathbf{E}$ ,  $\mathbf{B}$ ,  $\mathbf{J}$  of the vectors and  $\vec{G}_E$ ,  $\vec{G}_B$  of the tensors. Consider, a circular cylinder of radius  $R$  with conductivity  $\sigma_p$ , along the  $z$  axis of a cylindrical system of coordinates with unit vectors  $\hat{\rho}$ ,  $\hat{\phi}$ ,  $\hat{z}$ , embedded in a less conductive medium of conductivity  $\sigma$ . Thus, the local resistivity  $\rho_l$  is  $\rho_l = 1/\sigma_p$  for  $\rho \leq R$  and  $\rho_l = 1/\sigma$  for  $\rho > R$ . The expressions for  $\vec{G}_E$  and  $\vec{G}_B$  are, in general, very cumbersome. If we assume, however, that the current source coincides with the cylinder axis, we can obtain [8] the forms of  $\vec{G}_E \cdot \hat{z}$  and  $\vec{G}_B \cdot \hat{z}$  for  $\mathbf{r}' = (\mathbf{r}' \cdot \hat{z})\hat{z}$ . Their nonvanishing components are then found by a single Bessel function integration

$$\hat{z} \cdot \vec{G}_E \cdot \hat{z} = \frac{\rho_l}{R^3} \int_0^\infty n_l Z_0(\lambda, \rho; \omega) \cos\left(\lambda \frac{z}{R}\right) d\lambda, \quad (3)$$

$$\hat{\rho} \cdot \vec{G}_E \cdot \hat{z} = \frac{\rho_l}{R^3} \int_0^\infty Z_1(\lambda, \rho; \omega) \lambda \sin\left(\lambda \frac{z}{R}\right) d\lambda, \quad (4)$$

$$\hat{\phi} \cdot \vec{G}_B \cdot \hat{z} = \frac{\mu_0}{R^2} \int_0^\infty Z_1(\lambda, \rho; \omega) \cos\left(\lambda \frac{z}{R}\right) d\lambda, \quad (5)$$

where  $\mu_0$  is the magnetic permeability of vacuum,  $\rho = (\mathbf{r} - \mathbf{r}') \cdot \hat{\rho}$ ,  $z = (\mathbf{r} - \mathbf{r}') \cdot \hat{z}$ , and

$$Z_\nu = in_p \left[ H_\nu^{(1)}\left(n_p \frac{\rho}{R}\right) + A(\lambda, \omega) J_\nu\left(n_p \frac{\rho}{R}\right) \right], \quad \rho \leq R$$

$$= \frac{B(\lambda, \omega)}{\pi} H_\nu^{(1)}\left(n \frac{\rho}{R}\right), \quad \rho > R, \quad (6)$$

where  $J_\nu(w)$ ,  $H_\nu^{(1)}(w)$  are the Bessel and Hankel functions of the first kind and order  $\nu$ , respectively;  $n_l = \sqrt{i\mu_0\omega R^2/\rho_l - \lambda^2}$ . The functions  $A(\lambda, \omega)$  and  $B(\lambda, \omega)$  are [8]

$$A = \frac{\sigma_p n H_0^{(1)}(n) H_1^{(1)}(n_p) - \sigma n_p H_1^{(1)}(n) H_0^{(1)}(n_p)}{\sigma n_p J_0(n_p) H_1^{(1)}(n) - \sigma_p n J_1(n_p) H_0^{(1)}(n)}, \quad (7)$$

$$B = \frac{2n_p \sigma}{\sigma n_p J_0(n_p) H_1^{(1)}(n) - \sigma_p n J_1(n_p) H_0^{(1)}(n)}. \quad (8)$$

By numerically integrating Eqs. (3)–(5) with respect to  $\lambda$ , we can obtain the frequency domain solution from the convolution Eqs. (1) and (2). We then calculate the results in the time domain by inverse Fourier transform. In general Eqs. (3)–(5) can employ dispersive relations for  $\rho_l$ . However, as a first approximation [8], no frequency dependence was assumed.

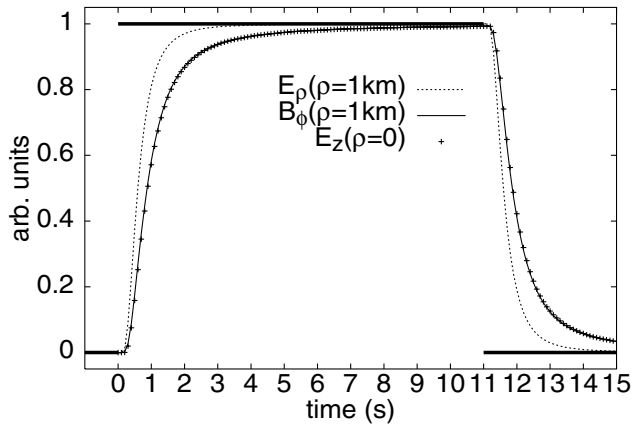


FIG. 4. A conductive cylinder embedded in a more resistive medium. A point current dipole source is located 80 km away and coincides with cylinder ( $z$ ) axis.  $E_z(\rho = 1 \text{ km})$  lies between  $B_\phi(\rho = 1 \text{ km})$  and  $E_z(\rho = 0)$  and hence not drawn. The thick line depicts the emitted pulse.

As an example, in Fig. 4, we consider a cylinder of resistivity  $2 \Omega\text{m}$  ( $= 1/\sigma_p$ , typical of a fault) with  $R = 500 \text{ m}$ , embedded in a medium of resistivity  $2000 \Omega\text{m}$  ( $= 1/\sigma$ , typical of the Earth's upper crust). The fields are studied 80 km far from the dipole source (i.e., comparable to the epicentral distance), at a point lying at a distance  $\rho = 1 \text{ km}$  from the cylinder axis, i.e., at  $\rho = 2R$ . A boxcar pulse with duration of 11 sec (i.e., comparable to the mean duration of the pulses in SES activities) is emitted. Two main results emerge: (i) Concerning the components of the electric field: The component  $E_\rho$  (i.e., perpendicular to the surface of the cylinder, associated with the accumulation of charges on the cylinder's surface) reaches its maximum value *earlier* than the component  $E_z$  (which, inside the cylinder, accompanies the high current density). (ii) Concerning the magnetic field  $B_\phi$  (measured again at  $\rho = 2R = 1 \text{ km}$ ,  $z = 80 \text{ km}$ ), it is practically simultaneous with  $E_z$  in the middle of the conductor, and their forms seem to coincide, as intuitively expected. In other words, the magnetic field  $B_\phi$  accompanies the high current density flowing inside the cylinder, which is "delayed" compared to the field  $E_\rho$  that signifies the accumulation of charges at the interface.

In the simple model above, no frequency dispersion of the dielectric constant was assumed and the results do show that the  $E_\rho$  field "precedes" the  $B_\phi$  field. However, a careful inspection of Fig. 4 reveals that the model cannot explain that the  $E$  field is recorded even before  $dB/dt$  (cf. the latter is not plotted). At this point, we recall the generalization of the Poynting theorem, as it applies to dielectric media [16,17].  $\mathbf{E} \times \mathbf{H}$  is the energy propagation vector *only* when  $\mathbf{D}$  is related to  $\mathbf{E}$ , and  $\mathbf{B}$  is related to  $\mathbf{H}$  according to the linear constitutive relations:  $\mathbf{D} = \epsilon_0 \vec{\kappa} \cdot \mathbf{E}$ ,  $\mathbf{B} = \mu_0 \vec{\mu} \cdot \mathbf{H}$ . When nonlinearities are included, it is expected that the conservation relation is in terms of

the action density. The generalized Poynting theorem [16] requires the inclusion of the contributions from both the electromagnetic field and the dielectric medium as well as their interaction in a single Lagrangian density. The total energy conservation then yields [16] 16 additional terms to the original  $\mathbf{E} \times \mathbf{H}$  Poynting vector. Such terms take care of nonlinear relations between  $\mathbf{E}$ ,  $\mathbf{B}$ ,  $\mathbf{D}$ , and  $\mathbf{H}$ , wave-vector dispersive interactions (those for which the constitutive relations would involve space derivatives of one or more of the fields, spatial dispersion), and interactions where magnetic effects are induced by electric variables and vice versa. Maybe, such nonlinear relations as well as wave-vector dispersive interactions should also be considered, beyond *criticality*, in order to achieve a satisfactory explanation of the present experimental results. This, however, still remains a challenge.

\*Electronic address: pvaro@otenet.gr

- [1] P. Varotsos *et al.*, Nature (London) **322**, 120 (1986).
- [2] P. Varotsos *et al.*, in *The Critical Review of VAN*, edited by Sir J. Lighthill (World Scientific, Singapore, 1996), p. 29.
- [3] S. Uyeda *et al.*, Proc. Natl. Acad. Sci. U.S.A. **97**, 4561 (2000); **99**, 7352 (2002).
- [4] P. Varotsos and K. Alexopoulos, *Thermodynamics of Point Defects and their Relation with Bulk Properties* (North-Holland, Amsterdam, 1986).
- [5] L. Slifkin, Tectonophysics **224**, 149 (1993); D. Lazarus, in *The Critical Review of VAN* [2], p. 91; F. Freund, J. Geophys. Res. **105(B5)**, 11001 (2000).
- [6] P. A. Varotsos, N. V. Sarlis, and E. S. Skordas, Phys. Rev. E **66**, 011902 (2002); **67**, 021109 (2003); **68**, 031106 (2003).
- [7] P. Varotsos, N. Sarlis, and E. Skordas, Proc. Jpn. Acad. Ser. B **77**, 87 (2001).
- [8] See EPAPS Document No. E-PRLTAO-91-007338 for a pdf file of additional information. A direct link to this document may be found in the online article's HTML reference section. The document may also be reached via the EPAPS homepage (<http://www.aip.org/pubservs/epaps.html>) or from <ftp.aip.org> in the directory /epaps/. See the EPAPS homepage for more information.
- [9] P. Varotsos, *The Physics of Seismic Electric Signals* (TERRAPUB, Tokyo, to be published).
- [10] P. Varotsos, N. Sarlis, and E. Skordas, Proc. Jpn. Acad. Ser. B **77**, 93 (2001).
- [11] E. Skordas *et al.*, Proc. Jpn. Acad. Ser. B **76**, 51 (2000).
- [12] P. Varotsos *et al.*, Phys. Rev. B **59**, 24 (1999); Acta Geophys. Pol. **48**, 263 (2000).
- [13] N. Sarlis and P. Varotsos, Acta Geophys. Pol. **49**, 277 (2001); J. Geodyn. **33**, 463 (2002).
- [14] P. Varotsos *et al.*, J. Appl. Phys. **83**, 60 (1998); Acta Geophys. Pol. **48**, 141 (2000).
- [15] N. Sarlis *et al.*, Geophys. Res. Lett. **26**, 3245 (1999).
- [16] D. F. Nelson, Phys. Rev. Lett. **76**, 4713 (1996).
- [17] D. F. Nelson and B. Chen, Phys. Rev. B **50**, 1023 (1994); R. Loudon *et al.*, Phys. Rev. E **55**, 1071 (1997); A. L. Ivanov and D. F. Nelson, Phys. Rev. B **58**, 1349 (1998); S. Glasgow *et al.*, Phys. Rev. E **64**, 046610 (2001).